

NOTES AND CORRESPONDENCE

The Moberly, Missouri, Tornado of 4 July 1995

PETE BROWNING

National Weather Service, Pleasant Hill, Missouri

JOHN F. WEAVER

NOAA/NESDIS/RAMM Branch, Colorado State University, Fort Collins, Colorado

BERNADETTE CONNELL

Cooperative Institute for Research in the Atmosphere, Colorado State University, Fort Collins, Colorado

20 July 1996 and 19 May 1997

ABSTRACT

Tornadic storms that occurred over northeastern Kansas and northern Missouri on 4 July 1995 are examined by combining the latest in National Weather Service technology with more routine datasets. The analysis provides an insightful description of the meteorological setting and evolution that led to the severe weather on this day. Strong thunderstorms first formed where an outflow boundary intersected a cold front, then new activity was triggered along the outflow boundary itself. It was found that small-scale outflow interactions may have played an important role in changing the nature of the convection already under way and were associated with the two most damaging tornadoes of the day. The case is also used to showcase how several new "modernization" datasets can be used together in a quickly accessible manner to provide a valuable and precise overview of a rapidly evolving meteorological event.

1. Introduction

Four July 1995 was an active severe weather day for residents of eastern Kansas and northern Missouri. During the early morning hours, severe thunderstorms produced damaging winds across the region. Later that afternoon another round of severe thunderstorms occurred, including several tornadic storms. A historic landmark schoolhouse was destroyed near the town of Linneus, Missouri, by one tornado, and another tornado struck the downtown business district of Moberly, Missouri. The Moberly tornado earned an F3 rating due to significant damage to both wood-frame houses and brick business structures. However, because it was the July Fourth holiday, few people were in the downtown district when the tornado struck. Also, a tornado watch and tornado warning had been issued well in advance of the tornado occurrence. Thus, no serious injuries or deaths occurred in what could have been a much more serious event.

As is often the case (e.g., Weaver and Purdom 1995), the 4 July 1995 episode was characterized by a large num-

ber of thunderstorms, among which only a small subset ended up producing tornadoes. At the same time, a large geographic region contained extremely unstable air and large values of forecast helicity. In this paper, the severe events over Missouri are examined using the latest in National Weather Service (NWS) technology: WSR-88D (Weather Surveillance Radar-1988, Doppler) radar data (available every 5 min), GOES-8 (Geostationary Operational Environmental Satellite) multichannel imagery (available for this case as often as every minute), National Centers for Environmental Prediction (NCEP) model analysis and forecast output (displayed using PCGRIDDs, an objective analysis software package that analyzes gridded data and presents it on a personal computer), as well as conventional observations. The combined use of these datasets provides an insightful description of the meteorological setting and evolution that led to the July Fourth tornadoes. This article does not present any new findings, but rather is used to illustrate how a combination of several new "modernization" datasets can be used in a quickly accessible manner to provide a valuable and precise overview of a rapidly evolving meteorological event.

2. Morning synoptic situation

Most forecasters are aware that upper flow over the central United States becomes relatively weak by July.

Corresponding author address: John F. Weaver, Research Meteorologist, NOAA/NESDIS/RAMM Branch, CIARA, Colorado State University, W. Laporte Ave., Fort Collins, CO 80523.
E-mail: weaver@cira.colostate.edu

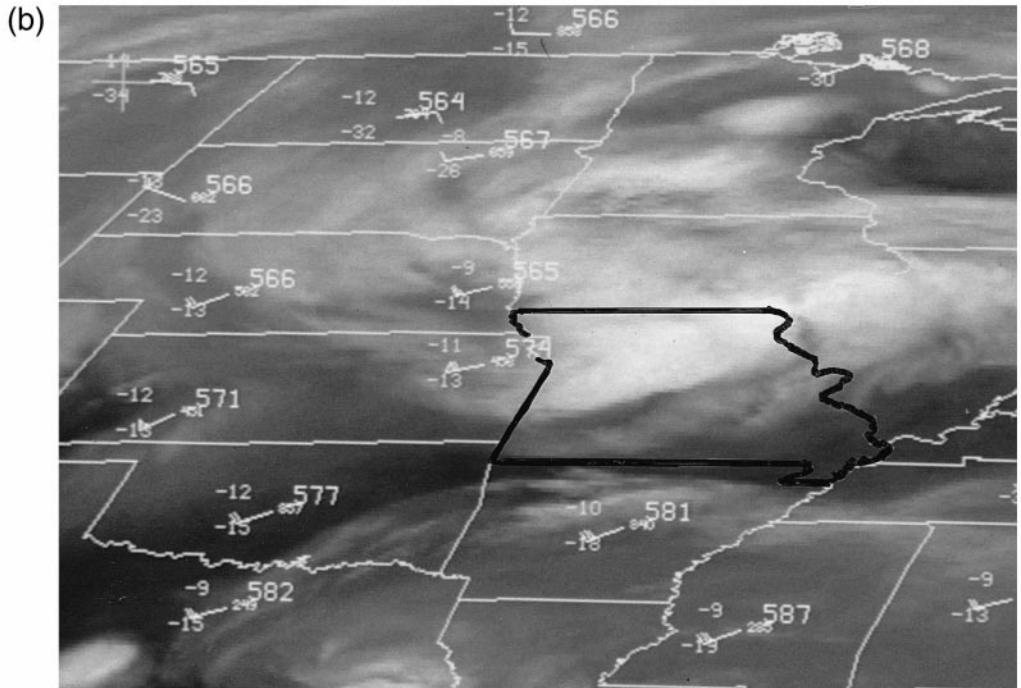
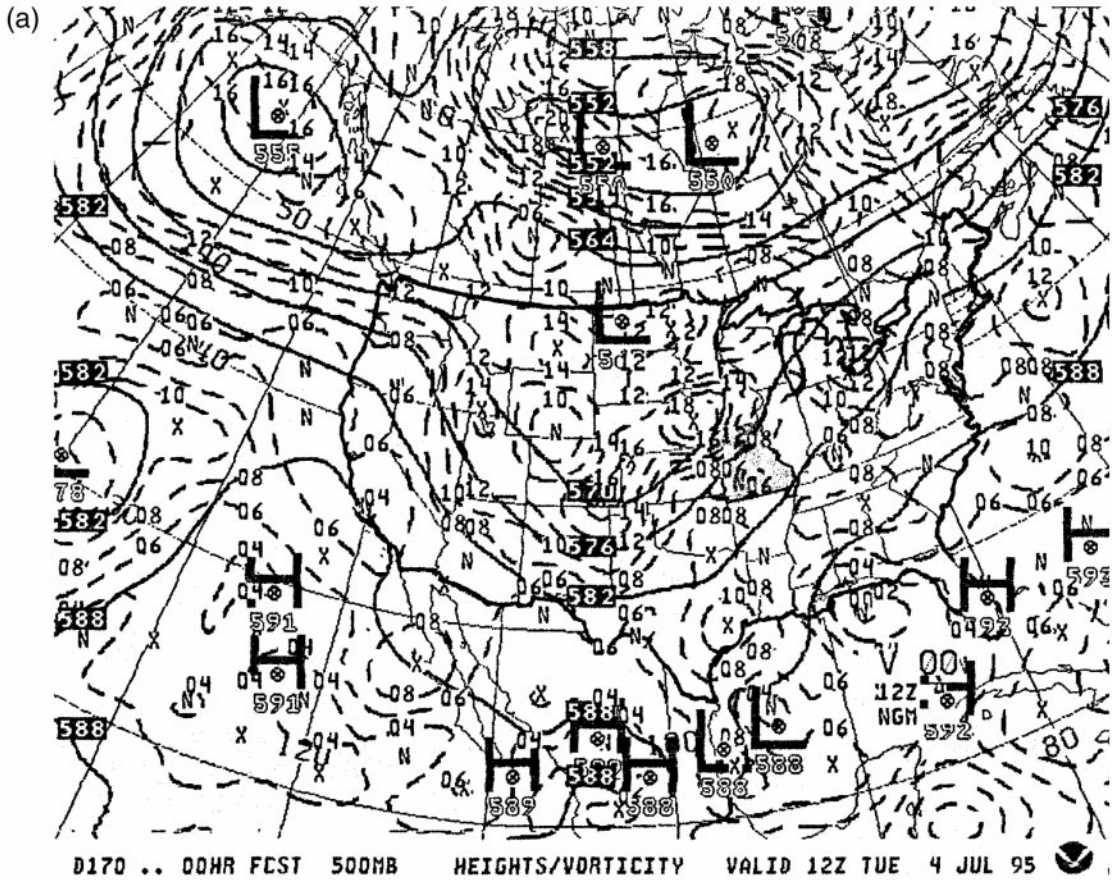


FIG. 1. (a) The 1200 UTC, 500-mb analysis on 4 July 1995 from the NGM initial analysis. Solid lines are heights in decameters; dashed represent vorticity in units of 10^{-5} s^{-1} . The border of the United States and Missouri are highlighted with shading; (b) $6.7\text{-}\mu\text{m}$ water vapor image taken over the central plains of the United States at 1145 UTC with 500-mb station plots overlaid. Missouri border in bold.

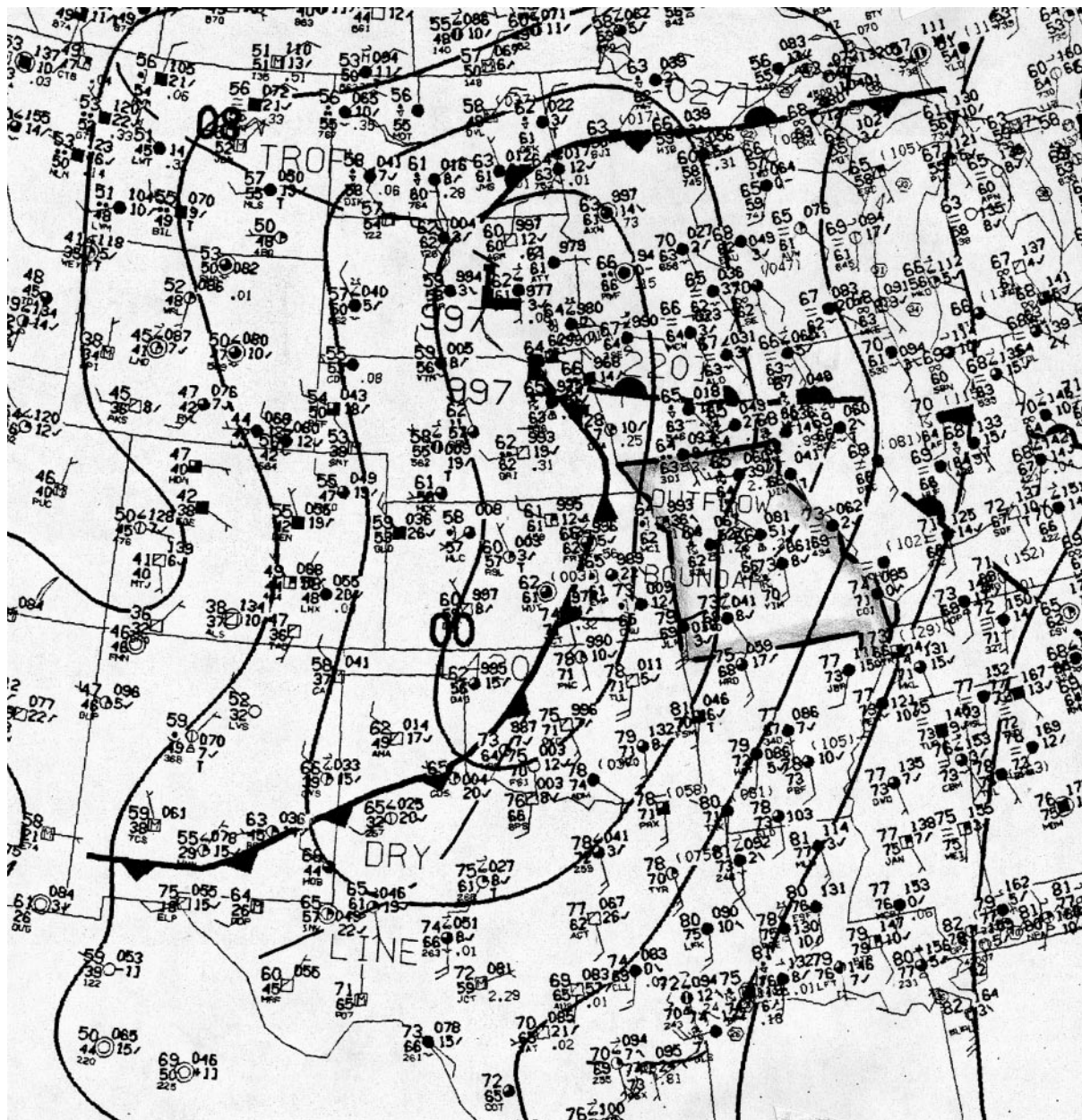


FIG. 2. The 1200 UTC surface analysis from 4 July 1995. Map is a copy of the facsimile chart transmitted routinely by NCEP. Station models are conventional U.S. plots. Border of Missouri is highlighted.

In fact, by late June the upper-tropospheric jet stream has typically migrated far to the north, and is found situated over the northern United States or southern Canada. The morning of 4 July 1995 found an exceptionally strong longwave trough centered over the central plains, with an intense jet as far south as New Mexico and western Texas. Maximum winds aloft were increasing and expected to be on the order of $30\text{--}40\text{ m s}^{-1}$ ($60\text{--}80\text{ kt}$) in the central plains by late afternoon. A combined look at the 500-mb analysis (Fig. 1a) and $6.7\text{-}\mu\text{m}$ wavelength satellite imagery (Fig. 1b) found at

least four embedded shortwaves within the larger trough. These included (a) an intense circulation in northern portions of Kansas and Missouri with an associated mesoscale convective system (MCS), (b) a circulation over southeast Colorado with an associated $16 \times 10^{-5}\text{ s}^{-1}$ vorticity max, (c) a relatively weak wave in Utah, and (d) a shortwave (and accompanying MCS) on the Texas–Louisiana Gulf Coast.

The longwave trough was amplifying with time and moving east-southeastward while the embedded shortwaves were traveling northeast through the longitudinal

flow. The combined effect of the various wave motions caused a nearly due eastward movement of the short-wave across northern Kansas, and a resulting eastward motion of the associated zones of synoptic-scale upward motion, which had provided support for the overnight convection. The shortwave trough crossed above, and parallel to, a quasi-stationary surface front.

The 1200 UTC surface analysis (Fig. 2) showed a cold front extending from a low pressure area in eastern portions of South Dakota and Nebraska, southward through eastern Kansas, then southwestward into western Oklahoma and Texas. An east–west-oriented warm front was situated over southern Iowa. (It was along this boundary where the overnight activity was occurring.) Numerical guidance suggested that the warm front would begin moving northward about midday and be well to the north of the region by late afternoon.

Soundings taken at 1200 UTC indicated a convectively unstable air mass. The lapse rate was nearly dry adiabatic between 800 and 500 mb in the warm sector over southwestern Missouri (Fig. 3a). With a forecast temperature/dewpoint of 29°C/21°C (85°F/70°F), the lowest kilometer, layer-averaged convective available potential energy (CAPE) was estimated at over 3000 J Kg⁻¹. By 1800 UTC (Fig. 3b), special soundings released in conjunction with a GOES-8 system test showed that the morning inversion had nearly mixed out and that the air mass was becoming even more unstable than earlier expected. Surface data found dewpoints in eastern Kansas and southern Missouri as high as 24°C (75°F). CAPE values exceeded 3500 J Kg⁻¹ and helicity was in the 100–200 m² s⁻² range.

The early morning convective outlook from the Severe Local Storms Branch of the National Severe Storms Forecast Center (now called the Storm Prediction Center) called for a moderate risk of severe thunderstorms across southern Kansas as well as southern and central Missouri. There was only a slight risk indicated for northern Missouri. However, a tornado watch (no. 703) was issued at 1815 UTC, which covered roughly the eastern quarter of Kansas, as well as most of western Missouri. A special update to the convective outlook, issued at 1853 UTC, placed eastern Kansas and most of the state of Missouri under a moderate risk of severe thunderstorms.

3. Late morning–early afternoon subsynoptic situation

a. Mid- to late morning

By midmorning, the Kansas–Missouri MCS had almost completely dissipated leaving behind a mesoscale, rain-stabilized air mass over Iowa and most of northern Missouri. Its southern edge was marked by a well-defined outflow boundary that extended across central Missouri into northeastern Kansas. Here, it intersected the cold front. This boundary could be seen on visible

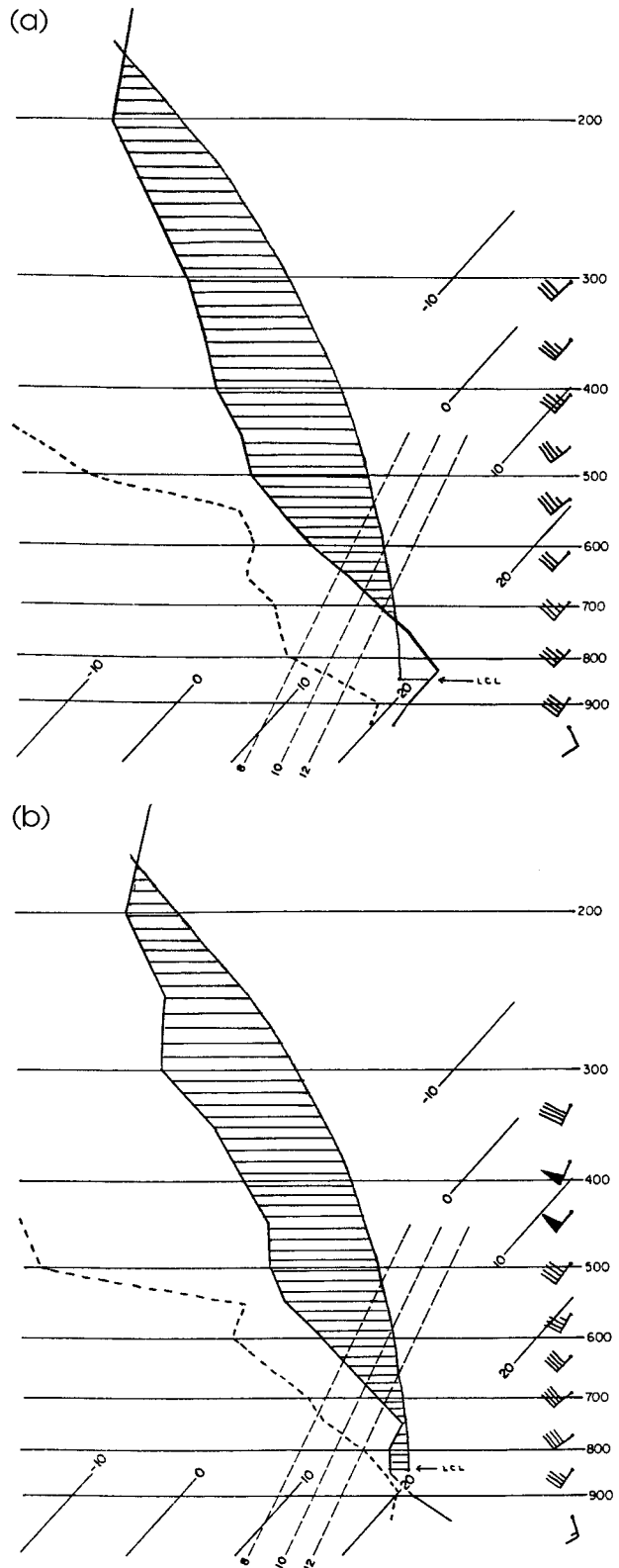


FIG. 3. (a) Springfield, MO, radiosonde taken at 1200 UTC 04 July 1995. Data are plotted on a Skew T–log p chart. Solid line is temperature; dashed dewpoint. Hatched area represents positively buoyant area for a parcel as defined in text. Wind barbs are plotted in kt, and (b) same as (a) except sounding released at 1800 UTC.

satellite imagery throughout the morning hours in the form of a well-defined arc cloud line (Fig. 4). The air-mass difference was evident all day in the surface θ_e fields, as defined by NCEP gridded RUC (Rapid Update Cycle) model output (Fig. 5). Thus, the early morning thunderstorm activity became a significant and unexpected factor in the weather later in the day. It had formed an air-mass discontinuity over central Missouri that otherwise would not have been there and that was not resolved by any of the standard model runs. As an example, note that the 6-h forecast from the Nested Grid Model (NGM, Fig. 6) finds the slow-moving warm front in southern Iowa but does not resolve the important outflow boundary.

A short line of weak thunderstorms developed during the mid- to late morning hours along a cloudy-versus-clear boundary in southwest Missouri (Fig. 4). That activity quickly moved northeast into the stable, rain-cooled region. The strongest of these storms was located where the new line intersected the outflow boundary. Though relatively short lived, this activity served to keep a portion of the stable air mass cloud covered, and cool.

b. Early afternoon

Just after noon local time, clusters of convection began forming in the warm sector east of the cold front and south of the outflow boundary (Fig. 7). The most dense coverage was found over eastern Oklahoma, eastern Texas, and southwest Missouri where low-level moisture convergence (analysis not shown) was strongest. Interestingly, the extreme western portion of the outflow boundary was edging slowly northeastward, as insolation began to destabilize part of the previously rain-stabilized air in northern Missouri; that is, destabilization and vertical mixing were allowing the boundary to erode. This destabilization is important for later convection in Missouri, which moves into northern portions of the state, since the region appears to be becoming more favorable with time.

While new convection was forming in and around the remnants of the mesoscale outflow boundary, the Kansas cold front was becoming more evident in both surface observations and visible satellite imagery. Animated imagery¹ reveals that convection developed just as the intense shortwave trough reached the front. This trough was moving toward the Pleasant Hill warning area, and would arrive there by mid- to late afternoon. It represented another factor in the short-range forecast time frame that required careful tracking: its position could be easily monitored using satellite imagery.

4. Afternoon development

The convective activity became more intense in northeast Kansas and northwest Missouri, with the strongest storms being those nearest the cold front-outflow boundary intersection. A short-lived tornado was reported by the Highland, Kansas, police department at 2035 UTC. By this time, the outflow boundary had become extremely diffuse on the visible satellite imagery. The arc cloud line had dissipated when the lower levels of the outflow region heated and mixed, and surface observations indicated southerly flow on both sides of the boundary. Also, there was no convergence evident on Doppler radar at this time. However, it is important to note that the hourly analysis of RUC surface output continued to find a strong gradient of θ_e (Fig. 8) and strong moisture convergence (not shown) in the vicinity of the boundary.

By midafternoon, the only remaining evidence of the outflow boundary on satellite imagery was an area of developing cumulus cloud streets south through southwest of the arc cloud line's last easily identifiable location, and patches of stratocumulus within a mostly clear area to the north (Fig. 9). A few congestus were developing near the western end of the unstable cumulus field, right along the discontinuity. The two regions of different cloud development, along with the congestus at the western edge of the line, allow the position of the diffuse boundary to continue to be monitorable on the imagery. As noted earlier, the discontinuity continued to show up on afternoon RUC analyses as strong gradients on the θ_e and moisture convergence maps.

Postevent analysis of 0.5° elevation angle WSR-88D reflectivity data showed a subtle line of weak echo associated with the outflow boundary, moving north-northeastward over the NWS Forecast Office at Pleasant Hill, Missouri. Being poorly defined, there is little chance that such a phenomenon would have been noticed on radar in real time. When outflow boundaries are newly formed, they typically appear as fine lines on radar reflectivity displays, arc cloud lines on satellite, and have associated wind shifts and temperature discontinuities. This boundary was not fresh and appeared as a brief hint of a diffuse line of slightly higher reflectivity in the animated reflectivity images.

New convection began to develop in west-central Missouri by early afternoon. The new activity initially formed about 30 km east of the Pleasant Hill radar, but quickly moved off toward the north-northeast at 18–21 m s⁻¹ (35–40 kt). Within a short time, the new activity moved beyond the 100-km optimal range,² just as a

¹ An electronic version of this paper containing animated loops can be found on the Web at 'http://www.cira.colostate.edu; select NOAA-NESDIS RAMM Team, then click on recent publication.'

² At the range of the three storms from both the EAX and LSX radars, the radar beam at 0.5° tilt would have been centered between 2400 and 3300 m above ground level. Thus, the radar beam would have been entirely above the boundary layer and could not have "seen" any of the important outflow interactions occurring at lower levels.

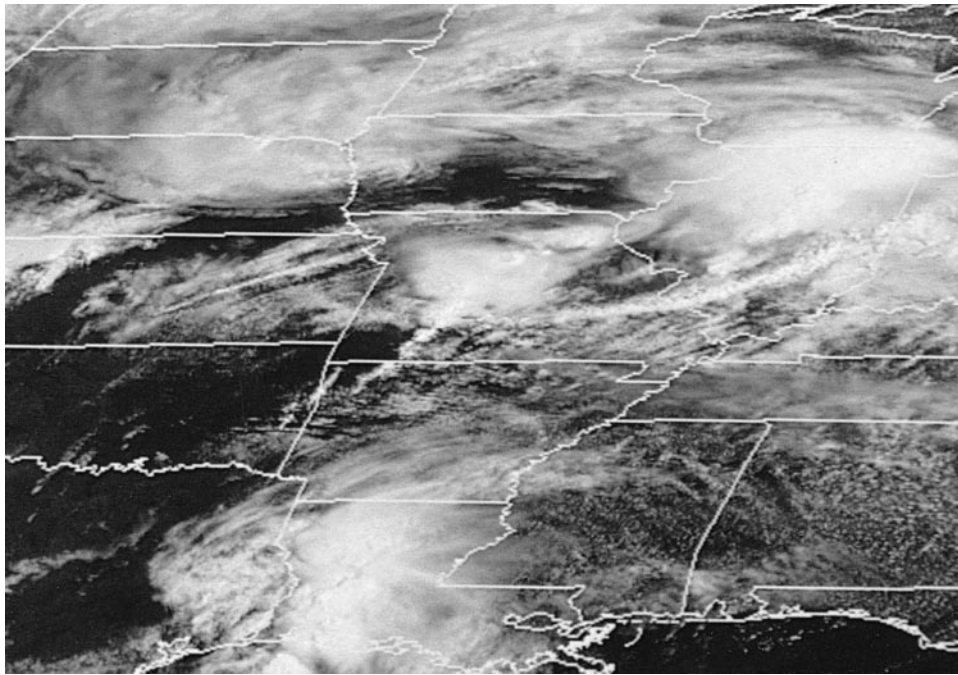


FIG. 4. The 1515 UTC visible satellite image showing the mesoscale outflow boundary discussed in text. The boundary is marked by the thin arc cloud line that stretches from eastern Illinois, through south-central Missouri, into extreme eastern Kansas.

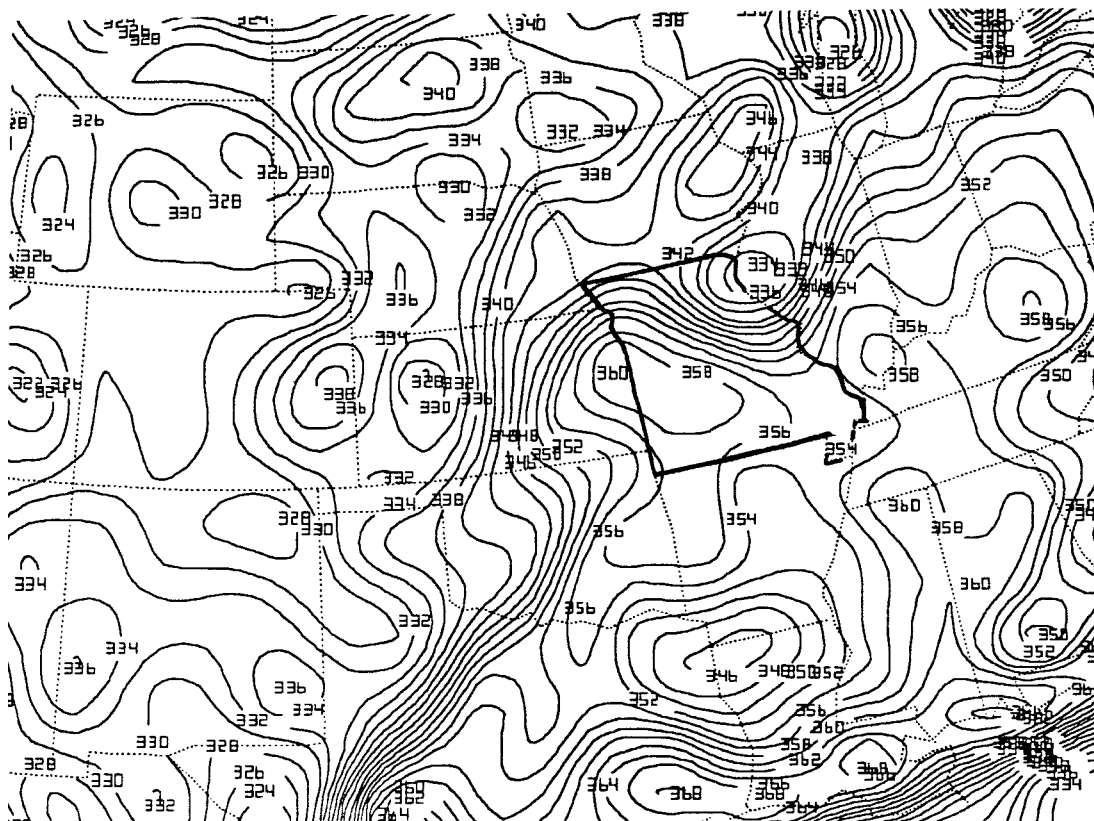


FIG. 5. Analysis of θ_e in kelvins based on PCGRIDDS analysis from 1900 UTC surface observations. Contours are in increments of 2 K. Missouri highlighted.

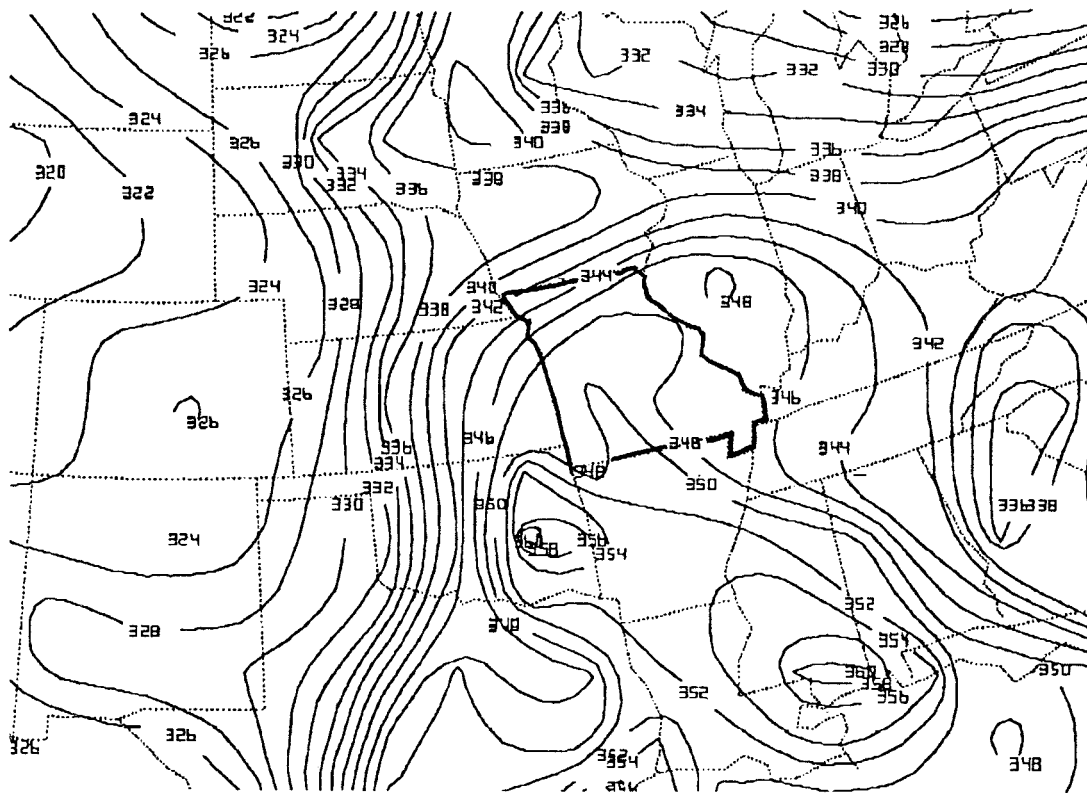


FIG. 6. The 6-h, NGM forecast of surface θ_s in kelvins. Forecast is valid for 1800 UTC 4 July 1995. Missouri highlighted.

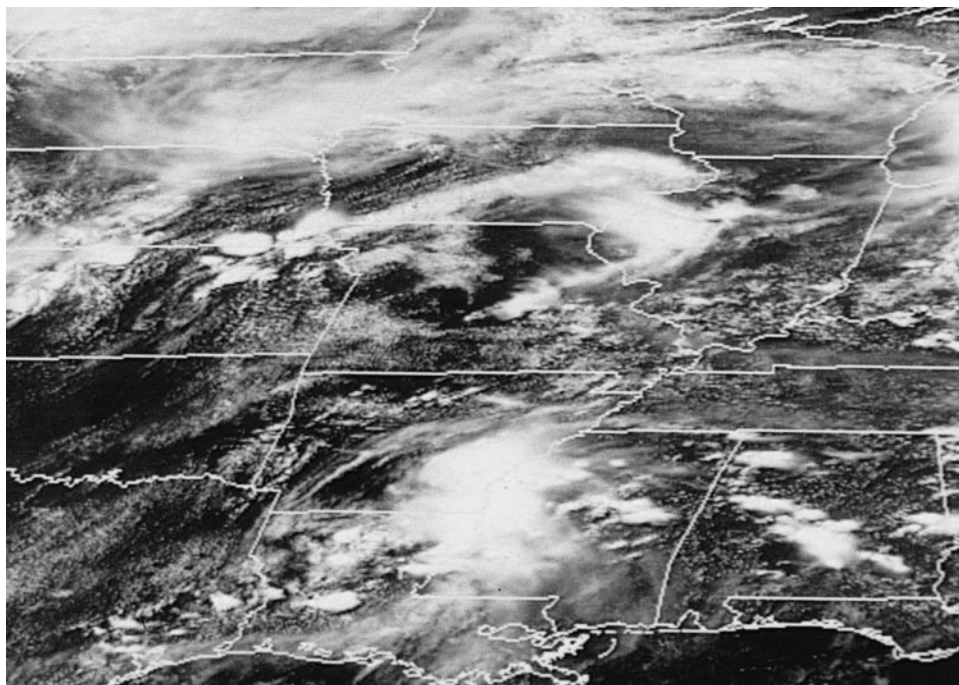


FIG. 7. GOES-8 visible satellite image from 1900 UTC 4 July 1995.

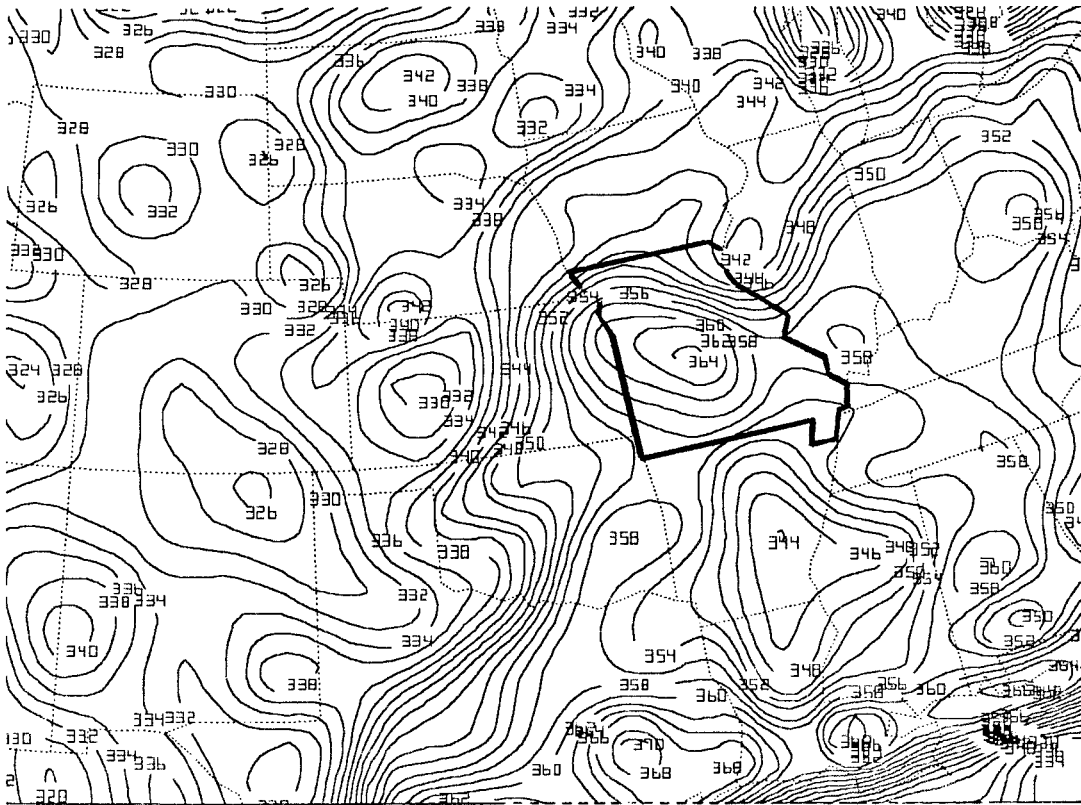


FIG. 8. Analysis of θ_e as in Fig. 5 except at 2100 UTC.

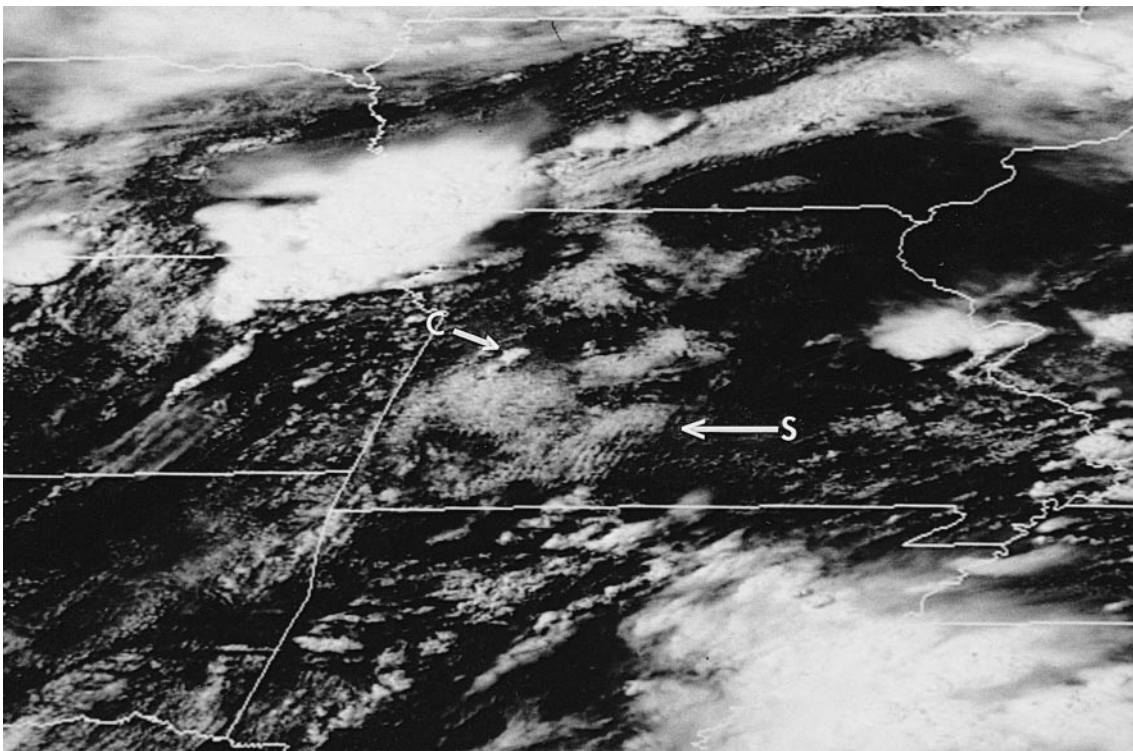


FIG. 9. Visible satellite image from 2025 UTC 4 July 1995 centered over north-central Missouri. Here, "S" indicates field of cumulus cloud streets, and "C" indicates a small cumulonimbus within the field of developing congestus in extreme western Missouri.

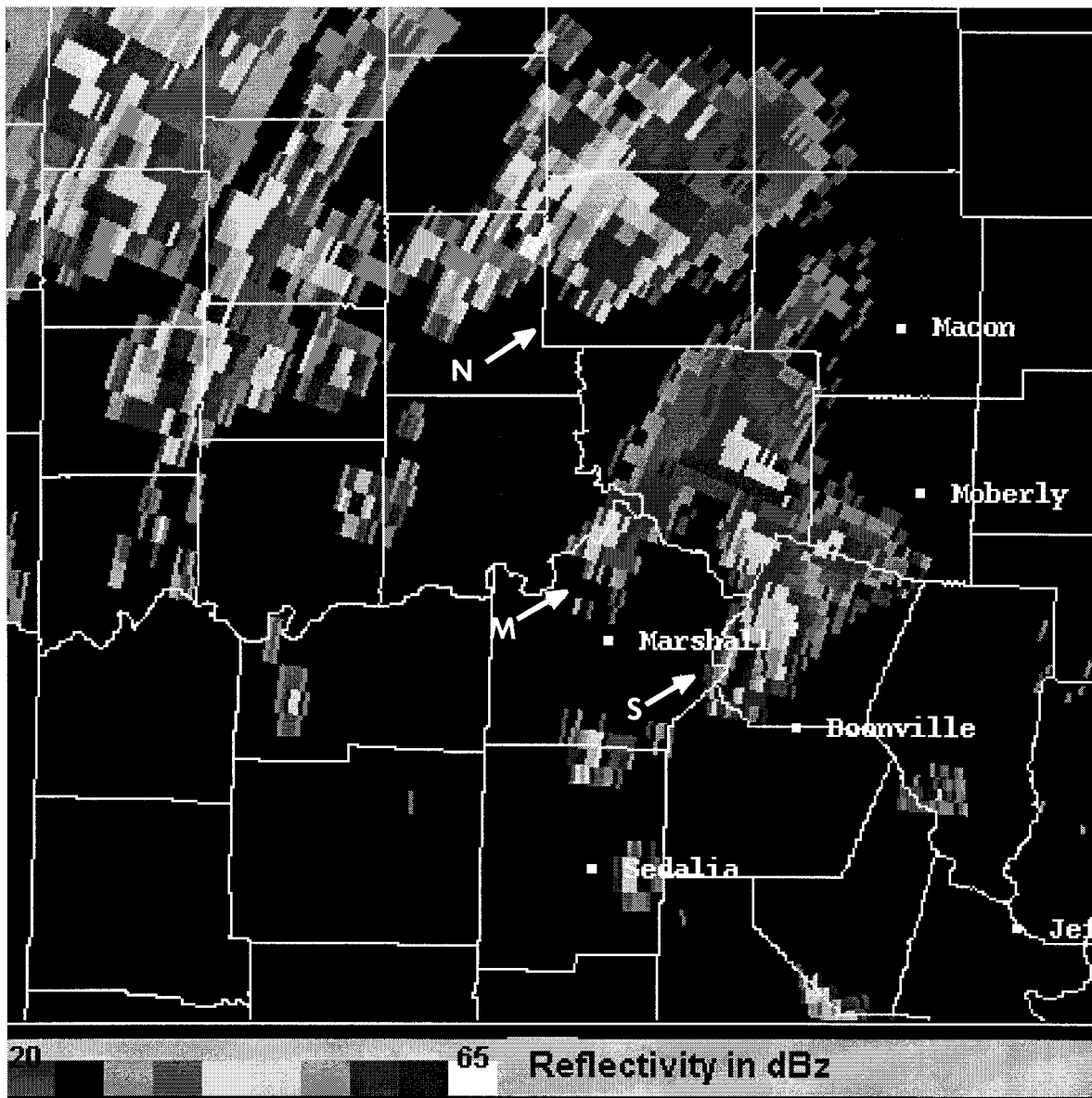


FIG. 10. Plan position indicator scan from the St. Louis, MO, WSR-88D radar (LSX) taken at 2241 UTC 4 July 1995. St. Louis vs Pleasant Hill data are shown, because that radar was slightly closer to the activity discussed and shows the three storms more clearly. Data are reflectivity, scanned at 0.5° elevation. The three cells described in text are indicated by arrows: "N" for the northern storm, "M" for the middle, and "S" for the southern.

complex evolution began, namely, (a) the northernmost storm intensified quite dramatically into a supercell with mesocyclone by 2241 UTC (feature "N" in Fig. 10), (b) the "middle" storm moved up between its two neighbors and began to weaken ("M" in Fig. 10), and (c) the southernmost storm grew relatively slowly with time ("S" in Fig. 10). On animated imagery, the center cell could be seen to move up between its two neighbors. As it did so, the reflectivity decreased appreciably. The storm was probably raining heavily at that point, and presumably producing a strong low-level outflow. However, there is no way to observe that from either the

Pleasant Hill (EAX) or St. Louis (LSX) radars in this case.

Satellite imagery makes the interaction clear. When the middle cell began to dissipate, small arc cloud lines appeared on both its north and south sides, visual indication that rain-stabilized air was rushing out to the north and south. Shortly after these short line segments merged with neighboring storms, important changes occurred. First, a short-lived F3 tornado developed beneath the northern cell near Linneus, Missouri, just after the outflow surge entered that storm's southern side. This is the tornado that destroyed the historic landmark

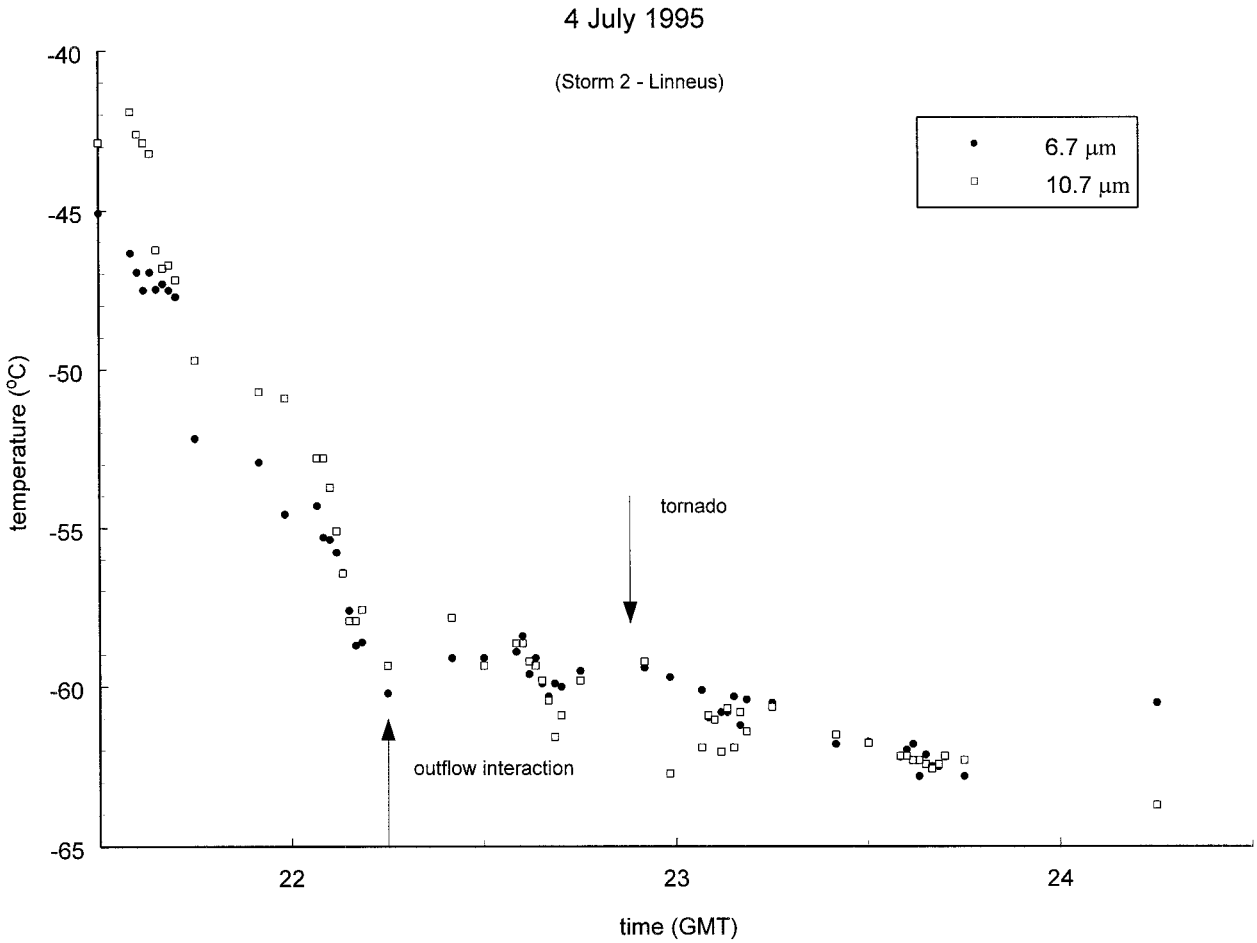


FIG. 11. Temperature histogram showing values of lowest cloud temperatures vs time for (a) the Linneus storm and (b) the Moberly storm. Solid dots are temperature minimums at storm top on the 6.7- μm channel; open boxes are for the 10.7 μm . Lowest temperatures are defined as the average of the coldest three anvil top values (to mitigate possible noise).

schoolhouse. Second, the overshooting dome of the southern storm (the storm approaching Moberly, Missouri) grew dramatically, with substantially lower temperatures developing on 10.7- μm infrared imagery. This occurred as the outflow surge entered its northern side. Figure 11 is a histogram of storm-top temperatures as sensed by both the 6.7 and 10.7- μm channels. The data indicate rapid cooling of the Moberly storm top occurring just after the interaction. Note that, for the Moberly storm, the 6.7- μm values are nearly always colder than the 10.7- μm . We interpret this to mean that there may have been a significant layer of moisture above the anvil.

Sequential imagery shows an interesting incident at this point in the evolution (Fig. 12). A small storm, which developed in a stratiform-covered region farther south of the referenced activity, died within 45 min of its inception (at approximately 2240 UTC) and put out a very small arc cloud line (“A” in Fig. 12a). This cloud line (and, presumably, a very small, rain-stabilized air mass) then moved north, reaching the southern storm (the Moberly cell) by 2330 UTC. The flanking “feeder”

towers on the south side of this storm (feature “b” in Fig. 12c) were observed to grow very rapidly over about a 5-min period. This evolution and southern flank feature are identical to the one discussed in Weaver and Purdom (1995) just prior to the touchdown of the F5 Hesston, Kansas, tornado of 13 March 1990. In this case, the Moberly tornado formed in something less than 10 min of the arrival of this very small scale outflow feature, although a rotating wall cloud had been reported by spotters for at least 30–45 min prior to the tornado formation. Super rapid scan (1-min intervals at times) image sequences provided unparalleled monitoring of the structure of this storm and the growth of the flanking towers. Rapid changes were also noted in the storm top with storm-relative loops showing strong divergence of cloud elements.

5. Summary and conclusions

In most cases, tornadic storms constitute a small subset of the thunderstorm activity occurring on a given

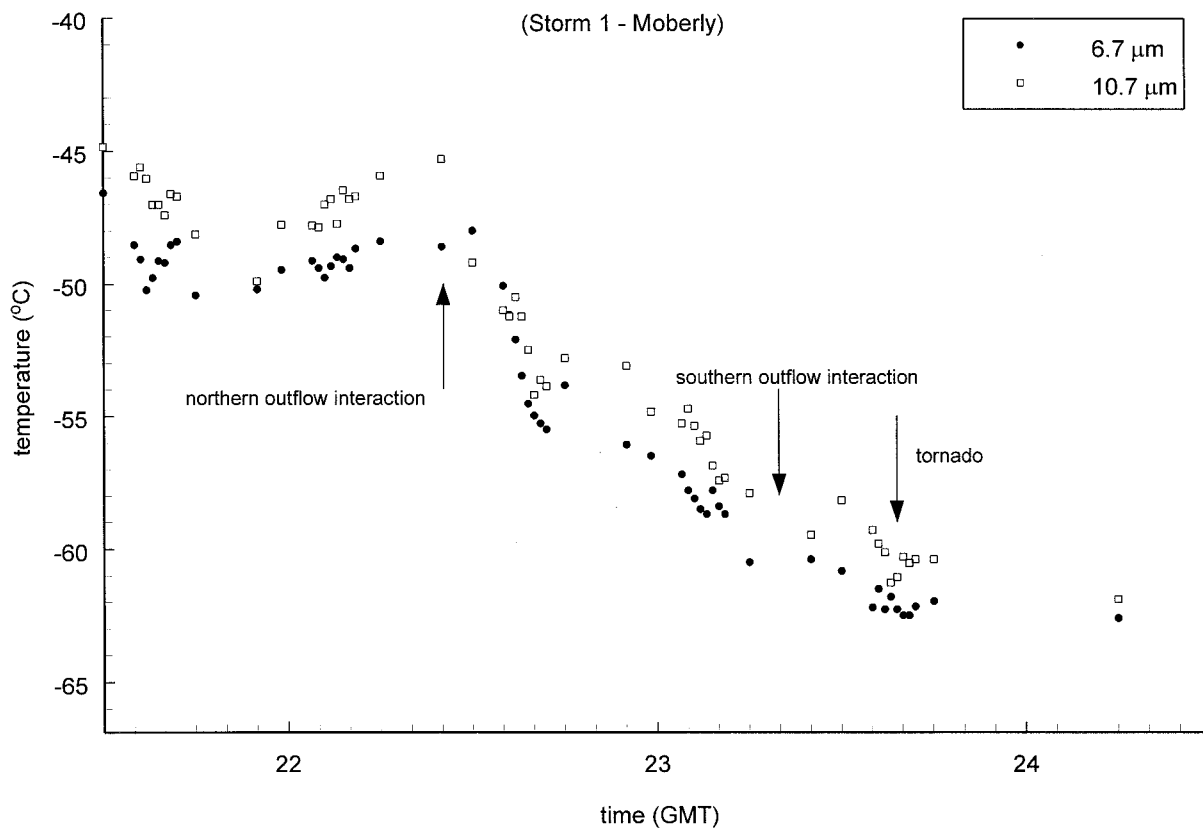


FIG. 11. (Continued)

tornado day (e.g., Weaver and Purdom 1995). It is often possible to identify these violent cells using Doppler radar alone. In the case of 4 July 1995, warnings based primarily on WSR-88D output were issued in advance of the tornadic damage in Moberly. However, such is not always the case. Even in the present instance, a broader understanding of the evolving mesoscale situation might have increased lead time somewhat on the Moberly storm.

Thunderstorms can alter their behavior appreciably upon interaction with other storms and preexisting boundaries (Purdom 1976; Weaver and Nelson 1982; Przybylinski et al. 1993; Weaver et al. 1994). Knowing that such features are present in the environment can provide the forecaster with valuable insight to supplement radar observations during tense severe weather warning operations. Doppler radar, when properly situated relative to the storm, provides the necessary real-time information about the evolving, internal thunderstorm structure. High-resolution digital satellite imagery can provide a “quick-glance” method for understanding why the storms are developing and evolving as they are and might provide a “heads up” on short-term intensification possibilities. Also, satellite combined with standard surface observations, model analysis, and other forecast data can define the setup conditions much better than either dataset alone. And while satellite imagery

by itself is useful for visually monitoring an evolving weather situation, the addition of derived analysis data can quantify resulting conclusions.

We have seen that the storms that produced tornadoes in this case were simply strong thunderstorms that became involved in interactions with other storms prior to tornadogenesis. The Pleasant Hill WSR-88D did reveal a mesocyclone prior to both tornadoes. Indeed, this was the key to the warnings issued for the storms. However, a recent study of mesocyclones detected on Doppler radar (Burgess et al. 1993) suggests that only about one-third of all mesocyclones produce tornadoes. That study’s lead author tells us (D. Burgess 1996, personal communication) that more recent studies indicate a ratio closer to 1:5, nationwide. Even in Oklahoma, during years with high tornado incident, the ratio is still somewhat less than 50% (Wood et al. 1996), and among these storms, only about one-third produced F2, or greater, tornadoes. It is important to reiterate that no tornado occurred in either the Linneus or the Moberly storms until storm interactions had taken place.

The role of very small scale interactions is unknown. Though not dynamically similar, one analog might be a deep, unstable snow field on an avalanche-prone slope. Some tiny factor, such as a small stone, or loud noise, can provide a trigger that then allows the full potential of the environment to be realized. Storm interactions

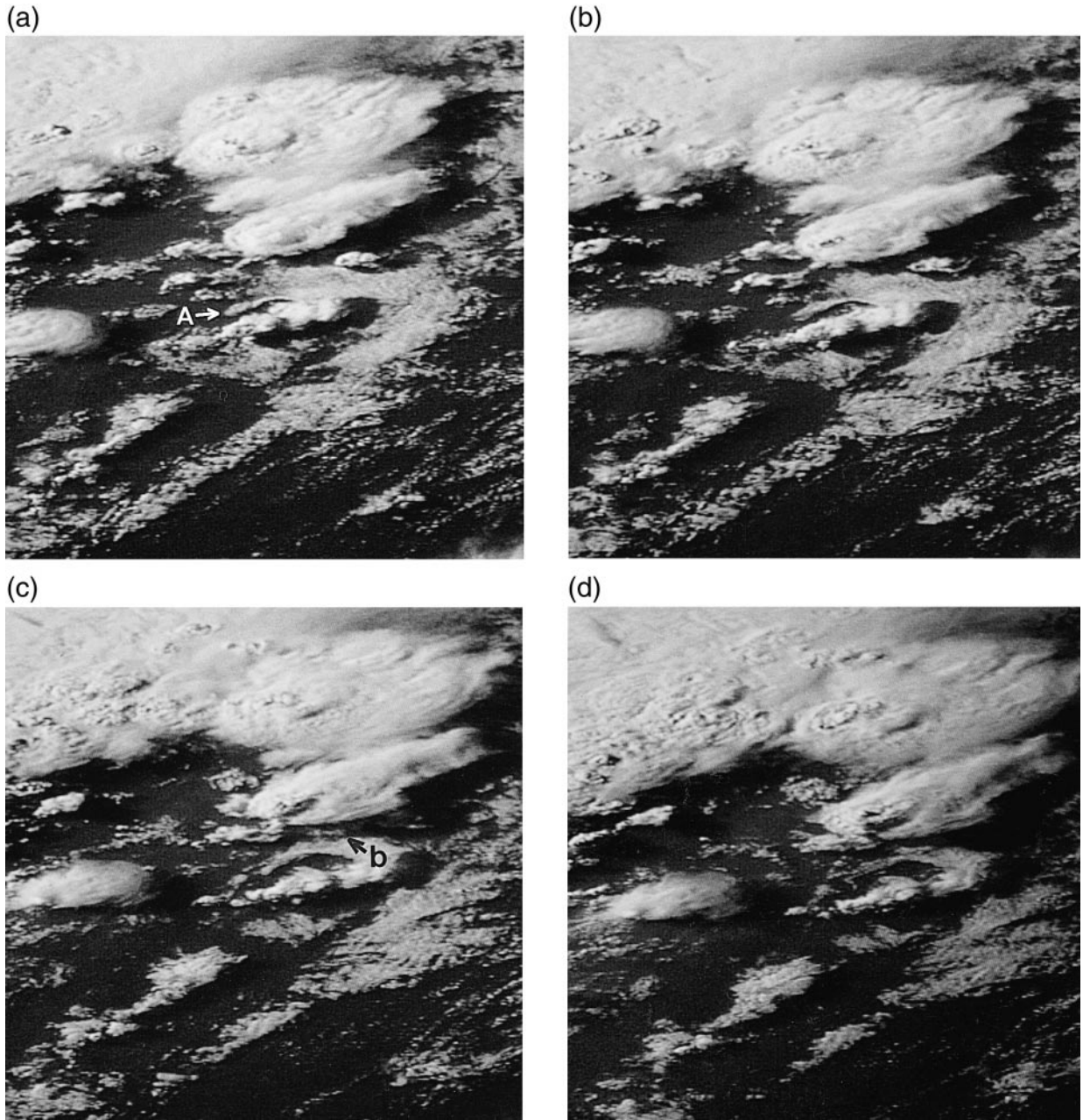


FIG. 12. Time series of visible imagery from the north-central Missouri taken on 4 July 1995: (a) at 2259 UTC, arrow "A" indicates small outflow that travels north toward the Moberly storm; (b) at 2308 UTC; (c) at 2315 UTC, arrow "b" indicates flanking towers on Moberly storm; and (d) at 2325 UTC.

that intensify storms or lead to tornadogenesis are not surprising (e.g., Davies-Jones and Brooks 1993 or Purdom 1993). What is disconcerting in the case of the Moberly interaction [as well as that which occurred with the Hesston, Kansas, F5 tornado; Weaver and Purdom (1995)] is the implication that sudden changes can occur on timescales much shorter than previously associated with tornado development. This case illustrates not only the utility of using Doppler radar and satellite together, but also demonstrates the need for these datasets to be

made available at time increments much shorter than are currently available in most NWS offices today.

We would like to emphasize that the purpose of this paper has been to illustrate how a combination of several new "modernization" datasets can be used in a quickly accessible manner to provide a valuable and precise overview of a rapidly evolving meteorological event. We also hope that the material will help in future decisions regarding satellite and radar data frequency available to the field forecaster. Neither our current un-

derstanding of the dynamical interactions taking place, nor current data frequencies allow the information to qualify as a reliable, new forecast technique. We hope that the cases presented will be of interest to some components of the theoretical research community.

Acknowledgments. A portion of the research for this study was performed under NOAA Grant NA37RJ0202. The authors would also like to thank the Office of Meteorology at NWS Headquarters and Central Region Scientific Services for supporting the Visiting Science and Operations Officer Program that led to this research.

REFERENCES

- Burgess, D. W., R. J. Donaldson Jr., and P. R. Desrochers, 1993: Tornado detection and warning by radar. *The Tornado: Its Structure, Dynamics, Prediction, and Hazards, Geophys. Monogr.*, No. 79, Amer. Geophys. Union, 637 pp.
- Davies-Jones, R., and H. Brooks, 1993: Mesocyclogenesis from a theoretical perspective. *The Tornado: Its Structure, Dynamics, Prediction, and Hazards, Geophys. Monogr.*, No. 79, Amer. Geophys. Union, 637 pp.
- Przybylinski, R. W., T. J. Shea, D. L. Perry, E. H. Goetsch, R. R. Csys, and N. E. Wescott, 1993: Doppler radar observations of high-precipitation supercells over the mid-Mississippi Valley region. Preprints, *17th Conf. on Severe Local Storms*, St. Louis, MO, Amer. Meteor. Soc., 158–163.
- Purdom, J. F. W., 1976: Some uses of high-resolution GOES imagery in the mesoscale forecasting of convection and its behavior. *Mon. Wea. Rev.*, **104**, 1474–1483.
- , 1993: Satellite observations of tornadic thunderstorms. *The Tornado: Its Structure, Dynamics, Prediction, and Hazards, Geophys. Monogr.*, No. 79, Amer. Geophys. Union, 637 pp.
- Weaver, J. F., and S. P. Nelson, 1982: Multiscale aspects of thunderstorm gustfronts and their effects on subsequent storm development. *Mon. Wea. Rev.*, **110**, 707–718.
- , and J. F. W. Purdom, 1995: An interesting mesoscale storm–environment interaction observed just prior to changes in severe storm behavior. *Wea. Forecasting*, **10**, 450–453.
- , —, and E. J. Szoke, 1994: Some mesoscale aspects of the 6 June 1990 Limon, Colorado, tornado case. *Wea. Forecasting*, **9**, 45–61.
- Wood, V. T., R. A. Brown, and D. W. Burgess, 1996: Duration and movement of mesocyclones associated with southern Great Plains thunderstorms. *Mon. Wea. Rev.*, **124**, 97–101.